Fixed-Time Target Tracking Control of Onboard Inertially Stabilized Visual Platform System

Ying Cai, Zhen Chang, Peijuan Li, Guangming Chen, Yiting Liu and Fangzheng Gao

Abstract—**The paper focuses on the target tracking control for the onboard inertially stabilized visual platform system of mobile robot. Firstly, mathematical modeling of the visual platform tracking control system is conducted. Then, a new visual tracking control algorithm based on fixed-time control technology is proposed to enhance the tracking speed and accuracy of moving targets. Rigorous theoretical analysis demonstrates that the target can be tracked within a fixed time even in the presence of external disturbances. That is, the moving target remains consistently within the camera's field of view during the robot's motion by controlling the rotation of visual platform.**

Index Terms—**visual platform, fixed-time, tracking control, mobile robot.**

I. Introduction

WITH the development of image processing and computer vision technology, visual sensors are increasingly being applied to the field of artificial intelligence, and visual servo control is also one of the core research topics in the field of machine vision. This technology is widely used in fields such as mobile robots and robotic arms, primarily adjusting and controlling the motion of robots based on the visual information captured by cameras [1–4]. However, in practical scenarios, the field of view of the camera is greatly limited, making research on the application of visual platform valuable. As a mechanical device for mounting and fixing cameras, the visual platform system primarily connects tracking targets with fixed facilities. Gimbals can expand the motion space of tracking targets through their own rotation [5, 6].

Currently, there are many studies on tracking control methods for visual platform systems in the literature. Reference [7] proposes a unified visual tracking adjustment controller for onboard visual platform systems, which ensures that the target is remained within the camera's field of view. Another dual-frame onboard visual platform control scheme based on visual feedback from image feature points is proposed in [8]. The key idea is to decouple the structure of the controller by measuring the camera's inertial angular velocity. The resulting controller can compensate for position errors caused by mutual movement between the visual platform and the object being measured. However, the velocities of both must be measured or estimated. Reference [9] explored an indirect robust control method, transforming the robust control design into an equivalent optimal control problem. This ensures that the stability of the visual platform tracking control system can also guarantee optimality. In Reference [10], the visual platform is fixed on the ceiling, and a finite-time tracking controller is designed based on visual feedback to control the robot to move along the desired trajectory. However, this situation leads to significant image delays and requires high camera performance.

It is worth noting that in the aforementioned studies on the application of visual platform for target tracking, some literature mentions visual platform being stationary. However, in practical applications, visual platform systems should be combined with mobile devices to accomplish target-tracking tasks. For target tracking control algorithms, some studies require measuring or estimating the relative velocity between the mobile device and the targets during the tracking process. Addressing the above issue, this paper first conducts mathematical modeling of target-tracking systems based on mobile robot-mounted visual platform. Subsequently, leveraging finite/fixed-time control theory [11–15], this paper devises a fixed-time target tracking controller, which guides the moving target towards the central position of the camera's field of view within a fixed time. Furthermore, it effectively mitigates diverse disturbances arising during the visual tracking process, thereby fulfilling the objective of target tracking.

II. Problem Description

A. Mobile robot-mounted visual platform

To achieve the tracking of moving targets, it is generally necessary to mount a visual platform system on a mobile robot. The onboard visual platform system mainly consists of the following parts: the mobile robot, the camera, and the multi-degree-of-freedom visual platform. With the continuous movement of the mobile robot and the interference of dynamic targets, the target's pixel coordinates in the camera's field of view converge to the desired position by controlling the rotation of the visual platform. This paper primarily focuses on the design of the visual platform system. In this system, the camera captures the target object during the tracking process, and obtains the pixel coordinates of the target object in the camera's field of view (u_0, v_m) as feedback signals. These coordinates are then compared

Manuscript received April 27, 2024; revised September 15, 2024.

This work was supported by Jiangsu Key R&D Project (BE2021016-5) and by the Qing Lan project of Jiangsu Province.

Ying Cai is a postgraduate student in the School of Automation of Nanjing Institute of Technology, Nanjing 211167, China (e-mail:y00450220407@njit.edu.cn).

Zhen Chang is a postgraduate student in the School of Automation of Nanjing Institute of Technology, Nanjing 211167, China (e-mail:y00450220449@njit.edu.cn).

Peijuan Li is an associate professor in the Industrial Center, Nanjing Institute of Technology, Nanjing 211167, China (e-mail:lpj4444@126.com).

Guangming Chen is an associate professor in the School of Automation, Nanjing Agricultural University, Nanjing 210095, China (e-mail: gmchen@njau.edu.cn).

Yiting Liu is an associate professor in the School of Automation, Nanjing Institute of Technology, Nanjing 211167, China (e-mail: gcdlyt1985@163.com).

Fangzheng Gao is a professor in the School of Automation, Nanjing Institute of Technology, Nanjing 211167, China (corresponding author, e-mail:gaofz@126.com).

with the desired pixel coordinates of the visual center point (u_0, v_0) to obtain the pixel deviation values (E_u, E_v). The visual platform's rotational angular velocities $\dot{x}$ and $\dot{y}$ is controlled by using the fixed-time target tracking controller In this paper, the selected visual platform has two degrees of freedom, enabling control of the camera's pitch angle β and yaw angle α and the direction of camera rotation downwards and to the left is defined as positive.

B. Fixed-time tracking control of moving targets based on visual platform

Visual platform tracking control means that the target object remains at the center of the camera by controlling the visual platform system using visual feedback signals. Clearly, from the perspective of control system performance, the time taken to lock onto the target and the tracking accuracy are two important performance indicators. Fixed-time tracking control refers to the ability to lock onto the target within a fixed time and to control it remaining at the center of the visual field.

C. Background Knowledge

Definition 1. Consider the nonlinear system

$$\dot{x} = f(t, x) \ \text{ with } f(t, 0) = 0, \quad x \in R^n, \tag{1}$$

where $f : R^+ \times R^n \to R^n$ is continuous with respect to x. The equilibrium $x = 0$ of the system is (globally) uniformly finite-time stable if it is uniformly Lyapunov stable and finite-time convergent. By "finite-time convergence," we mean: If, for any initial condition $x(t_0) \in R^n$ at any given initial time $t_0 \geq 0$, there is a settling time $T > 0$, such that every $x(t, t_0, x(t_0))$ of system (1) is defined with $x(t, t_0, x(t_0)) \in R^n/\{0\}$ for $t \in [t_0, T)$ and satisfies $\lim_{t\to T} x(t, t_0, x(t_0)) = 0$ and $x(t, t_0, x(t_0)) = 0$ for any $t \geq T$.

Lemma 1. Consider the nonlinear system described in (1). Suppose there is a C^1 function $V(t, x)$ defined on $R^+ \times R^n$, class K_∞ functions π_1 and π_2, real numbers $c > 0$ and $0 < \alpha < 1$, for $t \in [t_0, T)$ and $x \in \hat{U}$ such that

$$\pi_1(|x|) \leq V(t, x) \leq \pi_2(|x|), \forall t \geq t_0, \forall x \in R^n,$$

and

$$\dot{V}(t, x) + cV^\alpha(t, x) \leq 0, \forall t \geq t_0 \ , \forall x \in R^n.$$

Then, the origin of system (1) is globally finite-time stable with $T \leq \frac{V^{1-\alpha}(t_0, x(t_0))}{c(1-\alpha)}$ for initial condition $x(t_0) \in R^n$.

Definition 2. The origin of system (1) is said to be globally fixed-time stable if it is globally finite-time stable and the settling time function $T(x_0)$ is bounded, that is, there exists a positive constant T_{max} such that $T(x_0) \leq T_{max}$, $\forall x_0 \in R^n$.

Lemma 2. Consider the nonlinear system (1). Suppose there exist a C^1, positive definite and radially unbounded function $V(x) : R^n \to R$ and real numbers $c > 0$, $d > 0$, $0 < \alpha < 1$, $\gamma > 1$, such that

$$\dot{V}(x) \leq -cV^\alpha(x) - dV^\gamma(x), \ \ \forall x \in R^n.$$

Then, the origin of system (1) is globally fixed-time stable and the settling time $T(x_0)$ satisfies

$$T(x_0) \leq T_{max} := \frac{1}{c(1-\alpha)} + \frac{1}{d(\gamma - 1)}, \ \ \forall x_0 \in R^n.$$

Lemma 3. For any $x_i \in \boldsymbol{R}$, $i = (1, 2, \cdots, n)$, and a real number $p \in (0, 1]$, the following inequality holds.

$$(|x_1| + \cdots + |x_n|)^p \leqslant |x_1|^p + \cdots + |x_n|^p.$$

Lemma 4. For any positive real numbers c, d and any real-valued function $\pi(x, y) > 0$, one has

$$|x|^c|y|^d \leq \frac{c}{c+d}\pi(x, y)|x|^{c+d} + \frac{d}{c+d}\pi^{-c/d}(x, y)|y|^{c+d}.$$

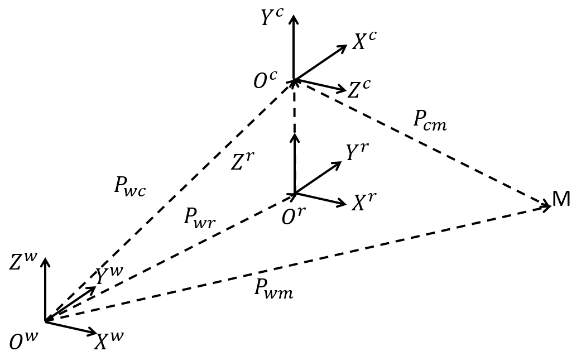

Fig. 1. Onboard visual platform coordinate system.

III. Main Results

To achieve our control objectives, relevant mathematical model is firstly conducted.

A. Mathematical model of mobile robot-mounted visual platform

The coordinate system of the onboard visual platform is shown in Fig.1. This platform involves three coordinate systems:

1) World coordinate system $W : O^w - X^wY^wZ^w$. In the world coordinate system, the coordinates of the moving target M are denoted as P^w_m. The origin coordinates of the robot coordinate system and the visual platform coordinate system are denoted as P^w_r,P^w_c.
2) Mobile robot coordinate system $R : O^r - X^rY^rZ^r$. Only consider the position of the robot in the plane $X^w - Y^w$. as $P^w_r = (x^w_r, y^w_r, \theta)^T$, where θ is the yaw angle of the mobile robot, i.e., the angle between the X^r axis and the X^w axis, with counterclockwise direction as positive; ω is the rotational angular velocity of the robot. Definition: φ represents the linear velocity of the mobile robot, which is in the same direction as the robot's X^r axis. Therefore, the three-axis linear velocity of the mobile robot relative to its coordinate system is $V_r = (v \cos\theta, v \sin\theta, 0)^T$.
3) Visual gimbal coordinate system $C : O^c - X^cY^cZ^c$. The coordinates of the visual platform relative to the robot coordinate system R are $P^r_c = (0, 0, h)^T$, where $h$is the height difference between the visual platform and the robot's center of mass. The position of the moving target M in the visual platform coordinate system C is $P^c_m = (x^c_m, y^c_m, z^c_m)^T$. Definition: The angular velocity of the visual platform relative to its coordinate system is $\Omega_c = (\omega_x, \omega_y, \omega_z)^T$, the linear velocity relative to its coordinate system is $V_c =$

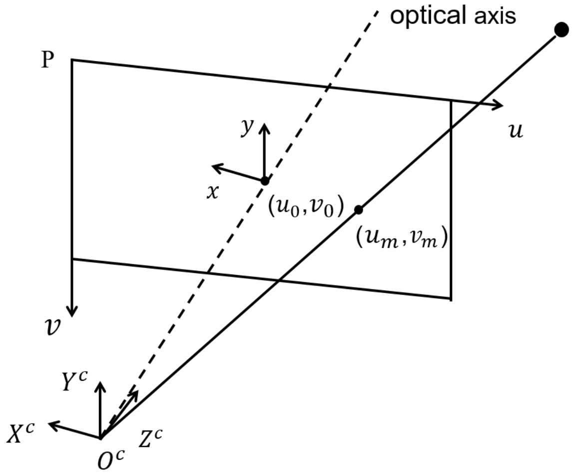

Fig. 2. Pinhole model of camera.

$(v_x, v_y, v_z)^{\mathrm{T}}$ and the angular velocity relative to the world coordinate system W is Ω_w.

Since the position feedback of the moving target M is based on the visual platform system, it is necessary to derive the coordinates of the moving target in the visual platform coordinate system C, denoted as P_m^c. As shown in Fig. 1,

$$P_m^c = (R_c^w)^{\mathrm{T}} \cdot p_{cm}, \tag{2}$$

The matrix R_c^w represents the rotation matrix from the visual platform coordinate system to the world coordinate system. According to the geometric relationship between the moving robot and the visual platform system, one has

$$\begin{aligned} p_{wc} &= p_{wr} + p_{rc}, \\ p_{wm} &= p_{wr} + p_{rc} + p_{cm}. \end{aligned} \tag{3}$$

The terms in Equation (2) are direction vectors in the world coordinate system, given by

$$\begin{aligned} &p_{wm} = P_m^w,\ p_{wr} = P_r^w, ‘p_{wc} = P_c^w, \\ &p_{rc} = R_r^w \cdot P_c^r,\ p_{cm} = R_c^w \cdot P_m^c. \end{aligned} \tag{4}$$

where the matrix R_r^w is the rotation matrix from the robot coordinate system to the world coordinate system, and the matrix R_c^w is the rotation matrix from the visual platform coordinate system to the world coordinate system. According to Equation (3), the following is derived.

$$p_{cm} = p_{wm} - p_{wc} = P_m^w - P_c^w. \tag{5}$$

Therefore, the coordinates of target M in the visual gimbal coordinate system C are obtained as:

$$P_m^c = (R_c^w)^{\mathrm{T}} \cdot (P_m^w - P_c^w). \tag{6}$$

The linear velocities of the visual platform and the mobile robot in the world coordinate system are:

$$\begin{aligned} \dot{P}_c^w &= R_c^w V_c, \\ \dot{P}_r^w &= R_r^w V_r. \end{aligned} \tag{7}$$

The mobile robot and the visual platform have a fixed height difference, so the relationship between the visual platform and the mobile robot in their respective coordinate systems is

$$V_c = R_r^c V_r. \tag{8}$$

The mathematical relationship between the rotation matrix of the visual platform to the world coordinate system and the angular velocity of thevisual platform is

$$\begin{aligned} \dot{R}_c^w &= \delta(\Omega_w) R_c^w, \\ \Omega_w &= R_c^w \Omega_c, \end{aligned} \tag{9}$$

where $\delta(\cdot)$ represents the skew-symmetric matrix. Combining equations (6)∼(9), the first-order derivative of the coordinates P_m^c can be obtained

$$\begin{aligned} \dot{P}_m^c &= -(R_c^w)^{\mathrm{T}}[\Omega_w \times (P_m^w - P_c^w)] + G(t) \\ &= \delta^{\mathrm{T}}(\Omega_c) P_m^c + G(t), \end{aligned} \tag{10}$$

where $G(t) = (R_c^w)^T \dot{P}_m^w - R_r^c V_r$.

B. Modeling and analysis of vision-based mobile target tracking control system

To track the moving target, it is necessary to obtain the position of the target object through the camera, which involves the pixel coordinate system $P : uv$. As shown in Fig. 2, the camera uses a pinhole model. The pixel coordinates of the moving target M in the pixel coordinate system P and the coordinates of the center point of the image plane are $(u_m, v_m)^{\mathrm{T}}$ and $(u_0, v_0)^{\mathrm{T}}$. The pixel coordinates of the target M can be determined

$$\begin{aligned} u_m &= u_0 - k\mu \frac{x_m^c}{z_m^c}, \\ v_m &= v_0 - k\mu \frac{y_m^c}{z_m^c}, \end{aligned} \tag{11}$$

where k and μ represent the pixel size and focal length of the camera, respectively. The system error is obtained by subtracting the coordinates of the moving target M on the camera imaging plane from the expected position.

$$E = (E_u, E_v)^{\mathrm{T}} = (u_0 - u_m, v_0 - v_m)^{\mathrm{T}}. \tag{12}$$

According to equation (10), we can obtain

$$\dot{E} = L_v(z_m^c) \dot{P}_m^c, \tag{13}$$

where

$$L_v(z_m^c) = \begin{bmatrix} \dfrac{k\mu}{z_m^c} & 0 & -\dfrac{E_u}{z_m^c} \\ 0 & \dfrac{k\mu}{z_m^c} & -\dfrac{E_v}{z_m^c} \end{bmatrix}.$$

Substituting the mathematical model of the visual platform (10) into equation (13), the error model for the vision-based target tracking control system is obtained.

$$\begin{aligned} \dot{E} = &\begin{bmatrix} \dfrac{E_u E_v}{k\mu} & -k\mu - \dfrac{E_u^2}{k\mu} \\ k\mu + \dfrac{E_v^2}{k\mu} & -\dfrac{E_u E_v}{k\mu} \end{bmatrix} \begin{bmatrix} \omega_x \\ \omega_y \end{bmatrix} + \\ &\begin{bmatrix} -\dfrac{q_z}{z_m^c} & \omega_z \\ -\omega_z & -\dfrac{q_z}{z_m^c} \end{bmatrix} \begin{bmatrix} E_u \\ E_v \end{bmatrix} + \begin{bmatrix} \frac{k\mu q_x}{z_m^c} \\ \frac{k\mu q_y}{z_m^c} \end{bmatrix}, \end{aligned} \tag{14}$$

The elements q_x,q_y and q_z represent the rows of vector $G(t)$. Due to the visual platform used in this paper being capable of controlling the camera's up-down and left-right movements, the angular velocities ω_x and ω_y of the camera are adjustable. Define $U = (\omega_x, \omega_y)\mathrm{T}$ as the input of the visual target tracking system. To simplify the expression, rearrange the system (14) as follows:

$$\dot{E} = L_u U + F(E,t) + D(t). \tag{15}$$

where

$$L_u = \begin{bmatrix} \frac{E_u E_v}{k\mu} & -k\mu - \frac{E_u^2}{k\mu} \\ k\mu + \frac{E_v^2}{k\mu} & -\frac{E_u E_v}{k\mu} \end{bmatrix};$$
$$F(E,t) = M(t)E = \begin{bmatrix} -\frac{q_z}{z_m^c} & \omega_z \\ -\omega_z & -\frac{q_z}{z_m^c} \end{bmatrix} E \tag{16}$$

are related uncertain disturbances to the system state.

$$D(t) = \left(\frac{k\mu q_x}{z_m^c}, \frac{k\mu q_y}{z_m^c} \right)^{\mathrm{T}} \tag{17}$$

is an external disturbance, i.e., disturbances caused by the motion of the robot and the target.

Remark 1. Considering the potential failure of target tracking due to rapid target movement and fast robot motion, it is assumed that both velocities are within a fixed range, meaning the variables $\dot{P}_m^w$ and V_r are bounded. At the same time, constrained by the real physical environment, the other environmental variables are also bounded. Assuming that the moving target M does not get too close to the visual platform, the depth information of the camera z_m^c does not tend to be zero. Therefore, it can be concluded that both disturbance terms $F(E,t)$ and $D(t)$ are bounded. The determinant of the L_u matrix in the target tracking control system (15) is $|L_u| = k^2\lambda^2 + E_u^2 + E_v^2 > 0$, hence its inverse matrix exists. Let $U = L_u^{-1}U^*$, then system (15) transforms into:

$$\dot{E} = U^* + F(E,t) + D(t). \tag{18}$$

Since the entire system model is two-dimensional, system (18) is split into:

$$\begin{aligned} \dot{E}_u &= u_1 + f_1(E,t) + d_1(t), \\ \dot{E}_v &= u_2 + f_2(E,t) + d_2(t). \end{aligned} \tag{19}$$

where $f_1(E,t)$ and $f_2(E,t)$ represent state disturbances, while $d_1(t)$ and $d_2(t)$ denote external disturbances. Similar in [16], the system satisfies the following assumption.

Assumption 1. System (19) satisfies

$$\begin{cases} |f_i(E,t)| \leqslant a_1|E_u| + a_2|E_v|, \\ |d_i(t)| \leqslant l < +\infty, \end{cases} \quad i = 1,2. \tag{20}$$

where a_1, a_2 and l are bounded constants.

C. Fixed-time tracking controller design

For the moving target tracking control system, the following controller is designed based on fixed-time control theory:

$$\begin{aligned} u_1 &= -k_{11}E_u^3 - k_{12}\mathrm{sign}(E_u), \\ u_2 &= -k_{21}E_v^3 - k_{22}\ \mathrm{sign}(E_v). \end{aligned} \tag{21}$$

To individually control the rotation of the two degrees of freedom of the visual gimbal, thereby controlling the camera's angular velocities ω_x and ω_y, where $k_{11}, k_{12}, k_{21}, k_{22} \in R^+$, and the controller parameters satisfy the following conditions:

$$\begin{aligned} &k_{12} = k_{22} = k' > l + \max\{k_{11}, k_{21}\}, \\ &k_{11} > \frac{3a_1 + a_2}{2}, \\ &k_{21} > \frac{a_1 + 3a_2}{2}. \end{aligned} \tag{22}$$

Theorem 1. For the target tracking control system model (15), if the controller is designed as (21) with the controller parameters satisfying (22), then the system is fixed-time stable, In other words, the system eventually ensures that the pixel errors E_u and E_v of the moving target M in the camera's field of view converge to 0 within a fixed time.

Proof Construct the Lyapunov function as

$$V = V_1 + V_2. \tag{23}$$

where $V_1 = E_u^2, V_2 = E_v^2$. Taking the derivative of V_1, yields:

$$\begin{aligned} \dot{V}_1 &= 2E_u\dot{E}_u \\ &= 2E_u(u_1 + f_1(E,t) + d_1(t)) \\ &\le -2k_{11}E_u^4 + 2a_1E_u^2 - 2k_{12}|E_u| \\ &\quad +2a_2|E_u||E_v| + 2|E_u|. \end{aligned} \tag{24}$$

Similarly, it can be obtained

$$\begin{aligned} \dot{V}_2 \le& -2k_{21}E_v^4 + 2a_2E_v^2 \\ &-2k_{22}|E_v| + 2a_1|E_u||E_v| + 2l|E_v|. \end{aligned} \tag{25}$$

From $V = V_1 + V_2$, it follows that

$$\begin{aligned} \dot{V} &= \dot{V}_1 + \dot{V}_2 \\ &\le -2(k_{11}E_u^4 - a_1E_u^2) - 2k_{12}|E_u| \\ &\quad -2(k_{21}E_v^4 - a_2E_v^2) - 2k_{22}|E_v| \\ &\quad +2(a_1 + a_2)|E_u||E_v| + 2l(|E_u| + |E_v|). \end{aligned} \tag{26}$$

By Lemma 4, it can be deduced that

$$|E_u||E_v| \le \frac{1}{2}|E_u|^2 + \frac{1}{2}|E_v|^2. \tag{27}$$

Multiplying both sides of equation (27) by $2(a_1 + a_2)$ and substituting into equation (26), it obtains that

$$\begin{aligned} \dot{V} \le& -2\Big(k_{11} - \frac{3a_1 + a_2}{2}\Big)E_u^4 \\ &-2\Big(k_{21} - \frac{a_1 + 3a_2}{2}\Big)E_v^4 - 2k_{12}|E_u| \\ &-2k_{22}|E_v| + 2l(|E_u| + |E_v|). \end{aligned} \tag{28}$$

Substituting the controller parameter condition (22) into the inequality (28), it obtains that

$$\dot{V} \le -c_1V^2 - 2(k - l)(|E_u| + |E_v|). \tag{29}$$

where parameter $c_1 > 0$ and

$$c_1 = \min\Big\{\Big(k_{11} - \frac{3a_1 + a_2}{2}\Big), \Big(k_{21} - \frac{a_1 + 3a_2}{2}\Big)\Big\}. \tag{30}$$

By Lemma 3, it follows

$$V^{\frac{1}{2}} = (|E_u|^2 + |E_v|^2)^{\frac{1}{2}} \le |E_u| + |E_v|. \tag{31}$$

Substituting equation (31) into (29), it obtains that

$$\dot{V} \le -c_1V^2 - c_2V^{\frac{1}{2}}, \tag{32}$$

where $c_2 = 2(k - l)$.

From equation (32) and Lemma 2, it can be concluded that the system is fixed-time stable, and the pixel errors E_u and E_v converge to 0 within a fixed time, which ensures that the target M reaches the center position of the camera's field of view.

IV. Simulation Analysis

Simulation experiments are conducted using Matlab software to build the system model and design the controller. The responses of E_u and E_v with the different initial conditions $(E_u(0), E_v(0)) = (2, 1)$ and $(E_u(0), E_v(0)) = (4, 2)$ are given in Figs. 3-4. From these figures, it is observed that all the closed-loop system states are regulated to zero in a fixed time, which accords with the main results established in Theorem 1 and also demonstrates the effectiveness of the control method proposed in this paper.

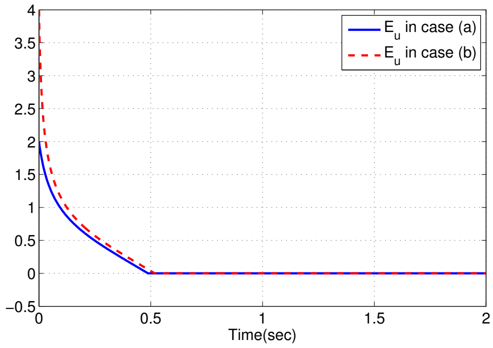

Fig. 3. Trajectories of E_u with the different initial conditions.

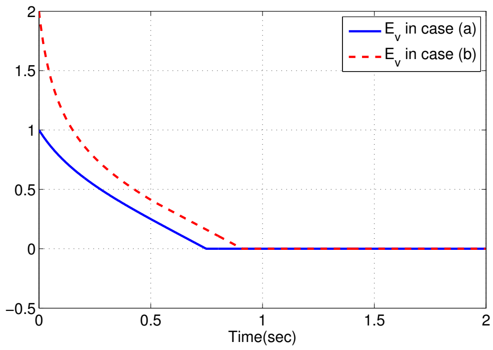

Fig. 4. Trajectories of E_v with the initial conditions.

V. Conclusion

This paper has addressed the problem of dynamic target tracking control under the scenario of onborne visual platform. The entire tracking system of the onboard inertially stabilized visual platform is modeled and analyzed firstly to derive the dynamic equations of the tracking control system. Subsequently, based on fixed-time control theory, a fixed-time target tracking controller is designed, which drives that the target can be tracked within a fixed time.

References

[1] Z. Gong, B. Tao, C. Qiu, Z. Yin, and H. Ding, "Trajectory planning with shortest path for modified uncalibrated visual servoing based on projective homography," *IEEE Transactions on Automation Science and Engineering*, vol. 17, no. 2, pp. 1076–1083, 2019.

[2] X. Zhang, Y. Fang, and N. Sun, "Visual servoing of mobile robots for posture stabilization: from theory to experiments," *International journal of robust and nonlinear control*, vol. 25, no. 1, pp. 1–15, 2015.

[3] S. Liu, W. Zhang, Y. Zhang, Z. Wang, and D. Gao, "A 3d semantic segmentation method for large-scale point cloud on deep learning." *Engineering Letters*, vol. 31, no. 4, pp. 1667–1674, 2023.

[4] Y. Luo, Y. Zeng, R. Lv, and W. Wang, "Dual-stream vo: Visual odometry based on lstm dual-stream convolutional neural network." *Engineering Letters*, vol. 30, no. 3, pp. 926–934, 2022.

[5] J. Yang, X. Liu, J. Sun, and S. Li, "Sampled-data robust visual servoing control for moving target tracking of an inertially stabilized platform with a measurement delay," *Automatica*, vol. 137, p. 110105, 2022.

[6] K. Deng, S. Cong, D. Kong, and H. Shen, "Discrete-time direct model reference adaptive control application in a high-precision inertially stabilized platform," *IEEE Transactions on Industrial Electronics*, vol. 66, no. 1, pp. 358–367, 2018.

[7] B. Li, Y. Fang, G. Hu, and X. Zhang, "Model-free unified tracking and regulation visual servoing of wheeled mobile robots," *IEEE Transactions on Control Systems Technology*, vol. 24, no. 4, pp. 1328–1339, 2015.

[8] Z. Hurák and M. Rezac, "Image-based pointing and tracking for inertially stabilized airborne camera platform," *IEEE Transactions on Control Systems Technology*, vol. 20, no. 5, pp. 1146–1159, 2011.

[9] A. Safa and R. Y. Abdolmalaki, "Robust output feedback tracking control for inertially stabilized platforms with matched and unmatched uncertainties," *IEEE Transactions on Control Systems Technology*, vol. 27, no. 1, pp. 118–131, 2017.

[10] M. Ou, S. Li, and C. Wang, "Finite-time tracking control for nonholonomic mobile robots based on visual servoing," *Asian journal of Control*, vol. 16, no. 3, pp. 679–691, 2014.

[11] Y. Shang, J. Huang, X. Shi, and X. Zhu, "Global finite-time stabilization for a class of upper-triangular systems subject to input saturation." *Engineering Letters*, vol. 28, no. 1, pp. 16–21, 2020.

[12] A. Polyakov, "Nonlinear feedback design for fixed-time stabilization of linear control systems," *IEEE transactions on Automatic Control*, vol. 57, no. 8, pp. 2106–2110, 2011.

[13] F. Gao, Y. Wu, Z. Zhang, and Y. Liu, "Global fixed-time stabilization for a class of switched nonlinear systems with general powers and its application," *Nonlinear Analysis: Hybrid Systems*, vol. 31, pp. 56–68, 2019.

[14] F. Gao, Y. Wu, and Z. Zhang, "Global fixed-time stabilization of switched nonlinear systems: A time-varying scaling transformation approach," *IEEE Transactions on Circuits and Systems II: Express Briefs*, vol. 66, no. 11, pp. 1890–1894, 2019.

[15] Z. Yang, Y. Zhao, and F. Gao, "Fixed-time stabilization for a wheeled mobile robot with actuator dead-zones," *IAENG International Journal of Computer Science*, vol. 48, no. 3, pp. 514–518, 2021.

[16] X. Sun, W. Zhu, H. Du, W. Chen, and C.-C. Chen, "Image-based fast finite-time target tracking control of onboard inertially stabilized camera platform," *IEEE Transactions on Industrial Electronics*, pp. 1–10, 2024.